NASA TTF-10,291

VELOCITY OF A PLASMA JET

F. B. Yurevich, M. V. Volk-Levanovich

NASA TTF-10,291

Translation of "Skorost' plazmennoy strui".
Vestsi Akademii Navuk Belaruskaya SSR, Seryya Fizika-Tekhnichnykh Navuk, No. 1, pp. 125-128, 1966.

NATIONAL AERONAUTICS AND SPACE ADMINISTRATION
WASHINGTON D.C. SEPTEMBER 1966

NASA TTF-10,291

VELOCITY OF A PLASMA JET

F. B. Yurevich, M. V. Volk-Levanovich

ABSTRACT

Discussion of a procedure for measuring the velocity of a plasma jet ejected from an electric-arc device. The procedure consists of recording brightness fluctuations of the jet, which for subsonic flows can be identified with the velocity of the jet.

In an investigation of plasma jets ejected from an electric-arc /125* device, the plasma jet velocity is an important parameter, along with temperature (enthalpy).

The problem of determining the velocity in this case is complicated by the fact that it is difficult to employ the probe methods, which are already known in gas dynamics, due to the high plasma jet temperatures. In addition, the probes contaminate the stream, distort the aerodynamic processes, and in the last analysis those disturbances which they introduce are measured.

In this connection, the method of brightness fluctuations is presently being employed to determine the velocity (Ref. 1, 2). The rate of change of the brightness fluctuations in subsonic flows can be identified with

---

* Note: Numbers in the margin indicate pagination in the original foreign text.

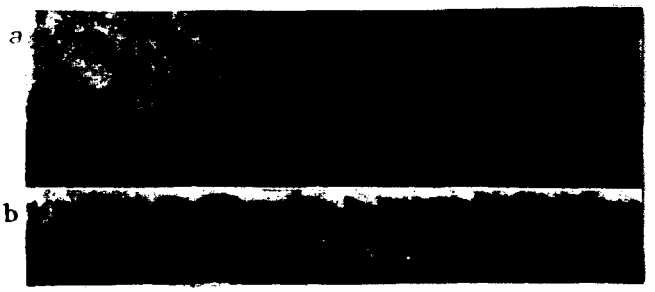

Figure 1

High-Speed Photorecording (HSP) of the Plasma Jet:

a - Regime No. 6 (with mixing chamber); b - Regime No. 8 (without mixing chamber).

the jet velocity.

The brightness fluctuation of the plasma jet is caused by the arcing mechanism in the plasmatron with vortical gas stabilization (Ref. 3).

The process is as follows. When the breakdown potential is reached between the electrode and the arc, the arc is closed at the wall, and the arc channel is bypassed by the shorter channel. Thus, between the two hot regions of the gas, there is a region which is heated to a lesser extent. Due to this fact, in spite of diffusion within the channel, the gas at the channel output consists of alternating regions which are relatively hotter and colder. The gas emittance changes sharply with a change in its temperature; therefore, brightness fluctuations must take place in the jet.

The velocity measurement according to the brightness fluctuations is based on the fact that the jet image turns in a direction which is perpendicular to the flow direction. Thus, the imprint of the brightness /126

fluctuations on the film is in the form of curves (Figure 1). The velocity of the process being studied can be computed according to the following formula (Ref. 1)

$$w = \frac{w_p}{\beta} \operatorname{tg} \varphi. \qquad (1)$$

Thus, for a specific linear scanning rate and image scale, the velocity measurement may be reduced to determining the angle of inclination of the brightness fluctuation line on the photogram.

In our case, this method of measuring the velocity according to the brightness fluctuations was employed to determine the plasma jet velocity at the plasmatron output with vortical gas stabilization of the arc. The construction and features of the type of plasmatron employed, with two cooled electrodes, were described in (Ref. 4). One distinguishing feature of the construction of the electric-arc device is the fact that both electrodes are welded. The inner diameter of the cathode is 20 mm; the inner diameter of the anode located at the plasmatron output is 15 mm.

For a wider variation in the plasma jet parameters, a mixing (damping) chamber was employed, along with the change in gas consumption and power. This chamber was in the form of a hollow, copper cylinder cooled with water, with an increased (at the electrode side) diameter (30 mm). The diameter of the output nozzle ($d_{out.}$) is given in the table of the function of the operational regime of the plasmatron device. A special gas ring, made of textolite and having two openings, was located between the anode and the mixing chamber. An additional

PARAMETERS OF THE PLASMATRON OPERATIONAL REGIME AND THE VELOCITIES OBTAINED EXPERIMENTALLY

Regime No.	ηN, kw	$d_{out.}$ mm	G_{N_2} g/sec	$G^{rel.}_{N_2}$ g/sec	$G^{add.}_{N_2}$ g/sec	$\overline{T}_{av}$ °K	$\overline{W}$ mean mass m/sec	W on the axis, m/sec
1	51	14	8.7	4.0	4.7	4200	720	680
2	58.2	14	6.5	4.0	2.5	5500	720	680
3	66.5	14	6.0	6.0	-	6000	800	810
4	77.0	14	5.5	5.5	-	6300	800	830
5	44.5	18	4.0	4.0	-	6200	340	350
6	53.2	14	5.0	5.0	-	6000	650	730
7	81.0	14	7.0	7.0	-	6000	900	1000
8	125	15	10.0	10.0	without mixing chamber	6200	11200	1900

supply of gas (nitrogen) was passed through these openings, and it was then mixed with the main flow of heated gas in the mixing chamber.

A high-speed photorecording device (HSP) (Ref. 5) was employed to measure the velocity; this device operated in the photorecorder regime. The rotation rate of the mirror was 3000-7500 rev/min, which corresponded to a linear scanning velocity of 150-375 m/sec. Since the movement of the film and the jet had to be perpendicular to each other, a specular turning system was employed. A RF-3 film was employed, with the sensitivity of 900-1200 inverse roentgens. In order to determine the image scale, a HSP camera was employed. In our case, the coefficient β equalled 0.37.

A special gauge was employed when the velocity distribution over the radius was measured. This gauge made it possible during the experiment to focus the HSP camera on a specific jet radius. Different cross-sections of the plasma jet, which were parallel to the axis, were delineated by a narrow slit (δ = 0.1 - 0.2 mm). It was assumed that the velocity measured at each point corresponded to the flow velocity at the center of the chord. Two factors pointed to this. In the first place, the utilization of the gauge made it possible to focus sharply on the plane passing through the jet axis and the center of the chord. In the second place, due to the fact that the temperature decreased sharply from the center to the periphery of the plasma jet, the maximum brightness corresponded to the chord center. /127

The jet velocity was measured for different plasmatron operational regimes, with the mixing chamber and without it. Figure 1 shows typical HSP-grams of the plasma jet at the output of the plasmatron. The difference in the nature of the jet, obtained with the mixing chamber (a) and without the mixing chamber (b), may be clearly seen. As would be expected, the mixing chamber smoothed out the brightness fluctuations very greatly.

The parameters of the plasmatron operational regime, the mean mass parameters of the jet obtained for them, and the experimental velocities on the axis are shown in the table.

The velocities on the jet axis are quite close to the values of the mean mass parameters computed according to the thermal balance. Regime No. 8 represents one exception to this, for which the velocity on the axis considerably exceeded the mean mass parameter.

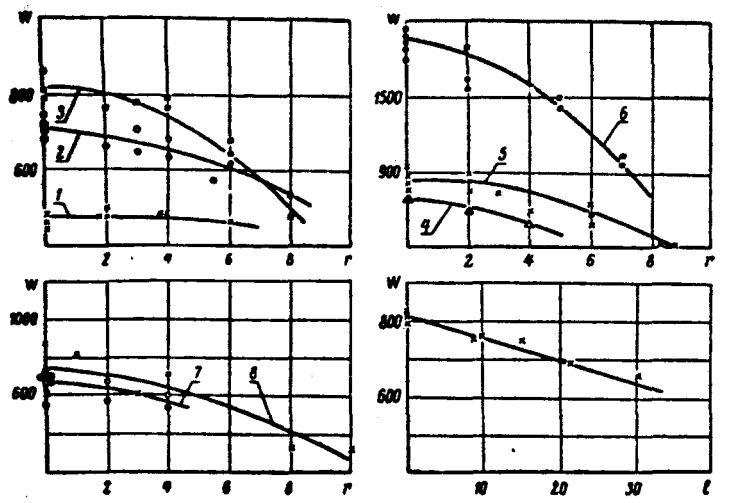

Figure 2

Velocity Distribution Over the Plasma Jet Radius at the Nozzle Output (1 - Regime No. 5; 2 - No. 3; 3 - No. 7; 4 - No. 2; 5 - No. 4; 6 - No. 8; 7 - No. 1; 8 - No. 6) and the Plasma Jet Velocity as a Function of the Distance to the Nozzle Section (Regime No. 3).

Figure 2 shows the velocity distribution along the jet radius at the nozzle output for different regimes. As may be seen from the figure, the velocity profile for the plasmatron operational regime without the mixing chamber is the steepest.

Graphs showing the velocity distribution in relative coordinates were compiled in order to compare the velocity profiles for different regimes. It was found that all of the curves thus obtained coincided in form, and 128 are closely described by the following expression, within the limits of experimental errors:

$$W = -0{,}4r^2 + 1. \qquad (2)$$

In addition to studying the velocity distribution over the jet radius,

we measured its value on the jet axis as a function of the distance to the nozzle section (Figure 2). There was a linear decrease in velocity on the axis with an increase in distance.

The accuracy with which the velocity is determined (Ref. 5) depends on the error entailed in measuring three quantities: rate of scanning, scale , and the angle ϕ. For the HSP camera, the error entailed in determining the scanning rate was $\pm$ 0.3%. The maximum relative error in determining the scale was - $\pm$0.2%. The greatest error was entailed in determining the angle ϕ, due to the large scatter of this quantity. In this connection, up to 40 values of the angle were taken for a more accurate determination on the HSP-gram. As a result, the accuracy with which the velocity was determined was $\pm$ 10%.

Notation

W -- rate of process being studied; W_p -- linear scanning rate; β -- image scale; ϕ -- angle of inclination of tangent to photoscanning curve; $\overline{W} = W/W_{axis}$ -- ratio of jet velocity on a given radius to velocity on the axis; $\overline{r} = r/r_0$ -- ratio of flow radius to radius of the output nozzle; ηN -- effective power; G -- gas consumption.

REFERENCES

1. Weiss, R. Z. Physik, 138, 11, 1954.
2. Strelkov, G. I., Yas'ko, O. I. Institut Fiziki Zhidkosti (IFZ), 3, No. 5, 93, 1960
3. Trokhan, A. M. Zhurnal Prikladnoy Mekhaniki i Tekhnicheskoy Fiziki, No. 2, 1964.

4. Sergeyev, V. L., Yurevich, Zh. B. IFZ, 7, No. 7, 1964

5. Dubovik, A. S. Photographic Recording of Rapid Processes (Fotograficheskaya registratsiya bystroprotekayushchikh protsessov), 1964.

BSSR Academy of Sciences
Institute of Heat and Mass Transfer

Received November 1, 1965

Scientific Translation Service
4849 Tocaloma Lane
La Canada, California